

**FAILURE OF COMPONENTS ALTHOUGH THE
CAUSES ARE SIMPLE & WELL DOCUMENTED**

Fahmida Hossain

James J. Scutti

Massachusetts Materials Research, Inc.

241 West Boylston Street

West Boylston, MA 01583

(508) 835-6262

1998

Abstract: For most of the materials commonly used in machinery, the static, fatigue and other design properties have been well-studied and documented. Yet, very common and simple oversights are made in choosing the right material and the correct design for an application, leading to premature failure of components in pieces of equipment. This paper will present two failures caused by inadequate design and improper material selection.

1) Failed pawls in hand operated winches for ladder hoist: A pawl finger is used in the winch which engages in-between the teeth of two gears to lock the winch in place when weight is on the ladder extension. Occasionally, the pawl sustains failure. Determination of the cause, as well as recommendations for improvements will be discussed.

2) Failed "Power Lock" Tapered Ring: This device was designed to fasten a sprocket to a shaft without the use of keyways. The power lock consisted to two tapered rings bolted together with six bolts, wedged against an outer and inner ring. One of the tapered rings fractured during a bench test. The root cause analysis and recommendations for prevention is provided.

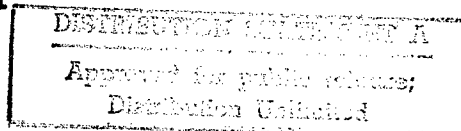
Key Words: Fatigue; inclusion; pawl; power lock; resulfurized; spring strip.

Failed Pawls in Hand Operated Winches for Ladder Hoist

Background: The hand operated winch to hoist ladders mainly operates with two gears. The "pawl" is a component in the piece of the equipment which engages in-between the teeth of the two gears to lock the winch in place, when hand cranking forces are released. Occasionally, the pawl is not properly engaged and is caught on the crest of the gear tooth. Then the reverse rotational forces bend the pawl as it jams the gears. The pawl finger was designed with a spring steel strip made from 301 stainless steel. This spring strip would allow some bending of the pawl finger when improperly engaged. But many failures of the pawl finger assembly had been reported.

Investigation: A few fractured pawls were examined to determine the root cause of the failure. Figure 1 shows a new pawl finger as viewed from one side. The spring plate is "sandwiched" in the bracket and the two sides of the bracket are welded in four locations (small arrows). The longer arrow is pointing to the pawl weight and the thicker arrow is showing the fulcrum bushing.

DTIC QUALITY INSPECTED 1



19980624 088

Binocular Microscope Examination: The spring strips always failed in an area that is unsupported by the bracket. Figure 2 presents an overall view of a failed pawl. Some plastic deformation was observed near the fractured surfaces of the spring strips.

Two samples, numbered 1 and 2, were selected for in-detail investigation. The overall view of the fracture surface for sample #1 is shown in Figure 3. Multiple origins were observed from the pawl weight side of the spring strip (small arrows). The “thumbnail shaped” features around the origins and relatively smooth fracture surface are typically associated with fractures that grow with operational time. The origins show radial markings emanating from them. The “thumbnail shaped” appearances radiating outward from the origins are macroscopic progression marks on a fracture surface which indicate positions of the advancing crack front. The final overload area was on the opposite side of the strip and measured approximately .004" in thickness (12% of the total thickness of the plate). This area is shown by the longer arrows in Figure 3.

The second sample also revealed similar features on the fracture surface but the origins were located on the opposite side or on the “flex” side of the spring.

Scanning Electron Microscopy: The fracture surfaces from the samples were examined at higher magnifications for determination of the fracture mode. The origins were always from the same side and from the surface. No anomalies were observed at or near the origins. Fatigue striations were visible emanating from the origins. Figure 4 presents an area with striations. Each striation indicates the position of the crack front after each succeeding cycle of stress or loading and are indicative of fatigue fracture.

Optical Microscopy: Cross-sections were made through the origins of the two fractured samples. No microstructural anomalies were found in the samples. The microstructure consisted of heavily worked elongated austenite grains, typical of full hard 301 stainless steel (SS). Figure 5 shows an overall view of the mounted cross-section through one of the origins of sample #1. The longer arrow shows the origin. The fracture was predominantly transgranular and showed many secondary cracks (small arrows). The small thicker arrows on the left-hand side of Figure 5 show initiations of other fatigue cracks, parallel to the fracture surface (FS).

A few cross-sections were made at the welds close to the failed spring strips; no microstructural change was observed on the strips near the welds.

Hardness and chemical analysis results meet the material specification requirements.

Conclusions and Discussion: The failed pawls fractured by fatigue in the center area of the spring strip. When the pawl fails to engage itself properly in-between the gear teeth, it experiences a significant amount of bending, causing permanent plastic deformation and locally damaging the spring metal. The material used for the spring strip, 301 stainless steel (full hard), is very notch sensitive. The magnitude of the applied cyclic vibrational forces on the spring strip when the pawl snaps off the top of the gear tooth

were large enough in the permanently bent areas to exceed the capability of the component and to initiate fatigue cracks. Continued use caused the fatigue cracks to grow to failure.

No material anomalies were observed. The welding performed on the pawl finger brackets was away from the fractures and the welding process did not contribute to the failures of the pawls.

Recommendations: We suggest a change in the shape of the tip of the pawl, which would be a retrofit to the existing pawls. Instead of the present rounded tip, the end should be ground so that the inner diameter side of the bracket makes an angle of about 40-45 degrees with the pawl weight side (outer diameter side) of the bracket (Figure 6). This reduces the contact area between the pawl tip and the gear tooth and the angled surface helps the pawl slide down to nest between the gear teeth. There is less chance of the pawl tip to get caught on the gear crest. The crests of the big gear teeth should be smoothed so that there are no burrs.

Alternative Materials for the Spring Strip: Other spring materials which can be used instead of the 301 SS are 410 SS and 420 SS, PH13-8Mo SS and Custom 450 SS. The 410 and 420 SS are martensitic in the hardened condition. They can be heat treated/tempered to the required mechanical strength. PH 13-8Mo and Custom 450 are precipitation hardenable stainless steels. These steels have better fatigue properties than the currently used cold-worked 301 SS. They also have good corrosion resistance and high strength and should serve the purpose when used in the pawl.

Failed "Power Lock" Tapered Ring

Background: A failed "Power Lock" device, used to fasten a sprocket to a shaft, consisted of two tapered rings (Ring A and Ring B) bolted together with six bolts holding an outer and inner ring. Ring A reportedly fractured during a bench test. The rings are made from SAE 1144 steel (a resulfurized grade).

Investigation

Binocular Microscopy: The Power Lock was disassembled, Figure 7, and examined with a binocular microscope. Cracks were observed on both sides of a drill hole in ring A, at the thinnest section. The arrow in Figure 7 is pointing to the crack. There were no cracks at any of the remaining drill holes.

The crack was broken open and the fracture surface was examined, Figure 8. The portion of the fracture surface on the "inside radius" (bottom surface in Figure 8) had a "woody" type fracture appearance, indicative of the longitudinal direction of the original bar stock. The portion of the fracture surface on the "outer radius" (top surface in Figure 8) in the thin section appeared "woody" and dull, measuring approximately $\frac{1}{4}$ ", and the thicker section (the remaining $\frac{1}{8}$ ") was shiny and rough. The "woody" appearance is typical of transverse fractures through cold drawn steel products. The drawing operation elongates

the grains improving the yield strength of the bar in the longitudinal direction, while reducing the transverse properties.

Scanning Electron Microscopy: High magnification examination of the outer radius fracture revealed that the thin end of the fracture had two “smooth” linear regions extending to the tip. Figure 9, at higher magnification, shows the tip of the fracture surface containing one of the smooth features. Energy dispersive x-ray spectroscopy was performed on the smooth linear portion and rough portion of the fracture surface. Analysis of the smooth surface revealed a major concentration of iron, minor concentrations of sulfur and manganese, and a trace of oxygen, indicative of a manganese sulfide inclusion. Analysis of the rough fracture surface revealed a major concentration of iron, and trace amounts of sulfur, manganese and oxygen indicative of the base steel material.

The rough “woody” features on the fracture surfaces are ductile, as shown by the dimple rupture in Figure 10. The thick end of the fracture, which appeared to be shiny and rough in our binocular examination, are “cleavage” facets, indicating a fast fracture, probably the last portion to separate.

Further SEM examination revealed the other fracture surface to be entirely dimpled rupture, similar to that shown in Figure 10.

Optical Microscopy: The failed ring was cross sectioned away from the fracture for microstructural analysis. Figure 11 shows the inclusions in the longitudinal cross-section. The inclusion content is quite significant and is typical for a resulfurized steel.

The chemical analysis and the hardness values meet the drawing requirements.

Conclusions and Discussion: The failure was caused by use of an inappropriate material. The large inclusion, comprised of manganese sulfide (a normal inclusion found in 1144, a “resulfurized” grade of steel) was observed at the origin of cracking at the thinnest section of tapered Ring A. The circumferential stresses applied to the ring during tightening created a crack and ultimately a rapid fracture of the ring. This was a fracture that occurred during a single application of load. No evidence of fatigue or other forms of “progressive” fracture were observed.

It is not known whether over torquing caused this particular failure. However, a large inclusion in an area of high stress/thinnest cross-section is more prone to fracture than another thicker area (under lower stress) and with smaller/fewer inclusion. The most adverse effects of non-metallic inclusions occur when the stress direction is perpendicular to the length of the inclusion and to the drawing direction, such as in the tapered rings.

The material meets the drawing requirements for 1144 steel, per ASTM A311. A relatively high inclusion content is normal for this grade of steel. Specifying the contents, sizes and shapes of inclusions is not applicable for “resulfurized” grades, per

ASTM A311. Therefore, when large, randomly distributed inclusions happen to be located at the thin portion of the tapered rings, failures can occur under normal torquing loads.

Recommendations: Since the tapered rings were stressed circumferentially, (i.e. transverse to the drawing direction), selection of a material with: 1) a low inclusion content, such as a non-resulfurized grade; and 2) fabricated by hot-rolling rather than cold drawing should improve the product.

If the Power Lock was to be used **at room temperature or above**, two steels that could be procured to meet the above criteria are: 1) ASTM A321 (equivalent to AISI/SAE 1055); and 2) ASTM A322, Grade 4130 (AISI/SAE 4130). Both steels should be procured in the annealed condition for machining. Note: The machinability of these steels is lower than that of 1144. After machining, the steels should be heat treated by austenitizing, quenching, and tempering to the drawing-specified hardness.

If the Power Lock was to be used in **cold** environments (i.e. 32°F or lower), then the steel selected must possess, in addition to the above criteria, adequate impact strength at -50°F. Steels such as the “high strength low alloy” (HSLA) grades per ASTM A633, or the ship hull steel HY-80 alloy can be used. The HSLA alloy A633 can be purchased, machined, and used in the normalized condition. The HY-80 must be austenitized, quenched and tempered after machining.

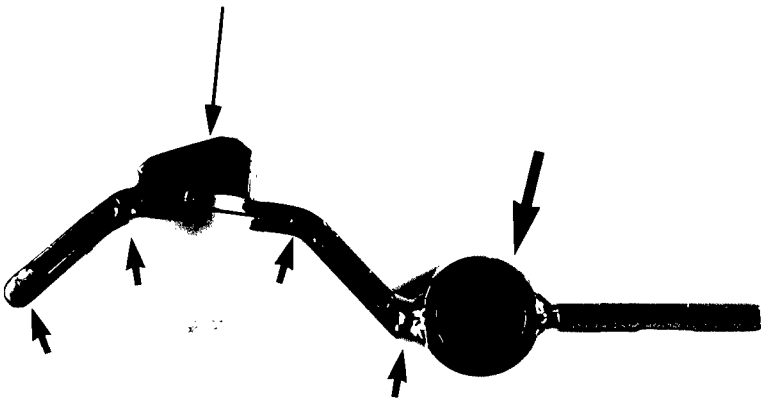


Figure 1. Overall view of a new pawl. Small arrows are pointing to the welded spots; the long thin arrow is showing the weight and the thick arrow is showing the fulcrum bushing. Mag. 0.6X

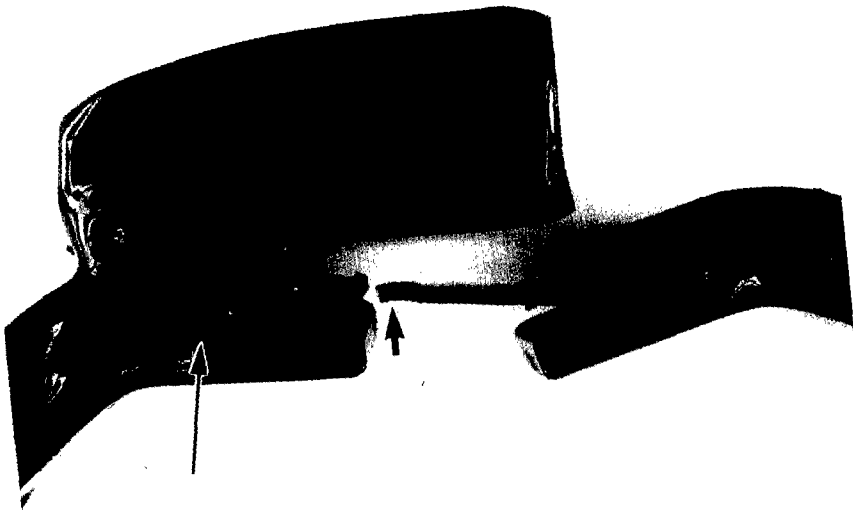


Figure 2. A fractured pawl; the smaller arrow is pointing to the plastic deformation and the longer arrow is showing the cracked weld. Mag. 2.2X



Figure 3. Overall view of the fracture surface of sample #1. Small arrows are pointing to the origins, longer arrows are showing the overload area. Mag. 6.4X

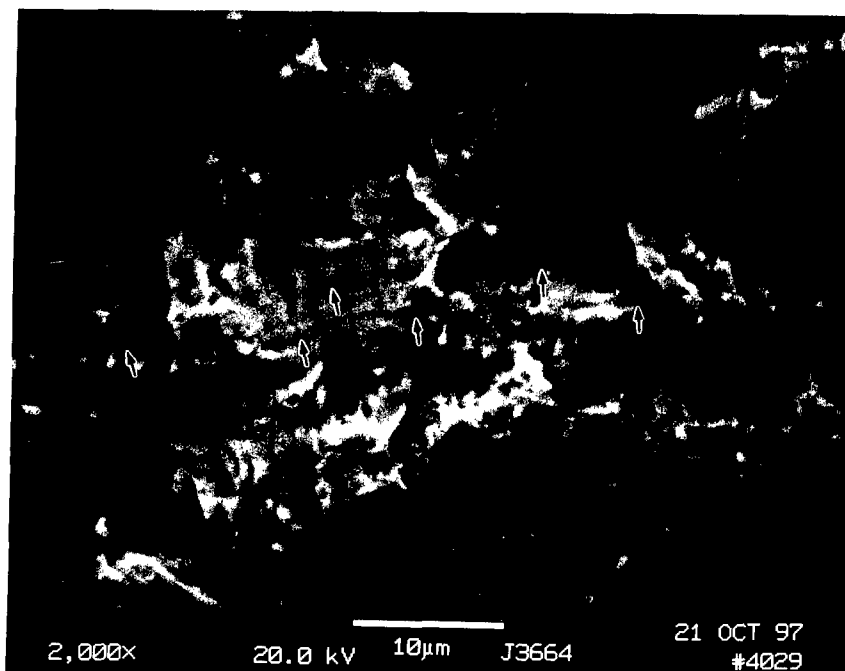


Figure 4. Higher magnification SEM photograph revealing fatigue striations (arrows) emanating from one of the origins. Mag. 2,000X

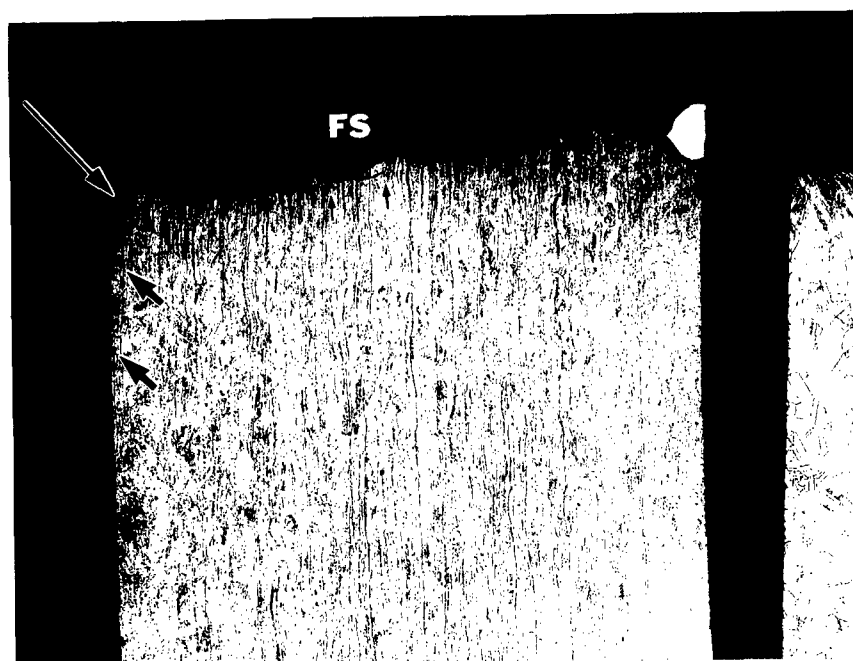


Figure 5. Mounted cross-section through one of the origins of sample #1. The longer arrow is pointing to the origin; small arrows are showing the secondary cracks on the FS. Thick small arrows on the left-hand side are showing other fatigue cracks initiating. Mag. 100X

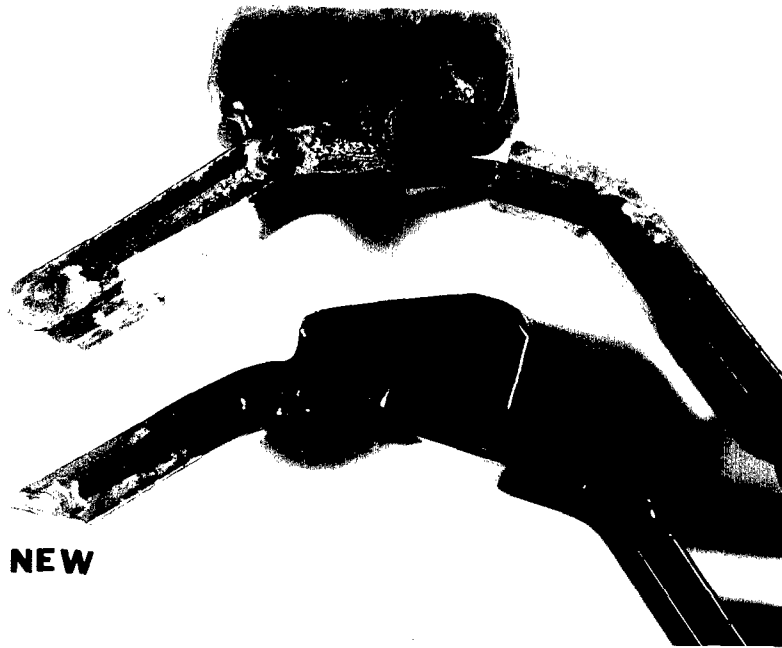


Figure 6. Suggested new pawl tip design for the existing pawls. The upper pawl is showing the tip design currently in use. Mag. 1.25X

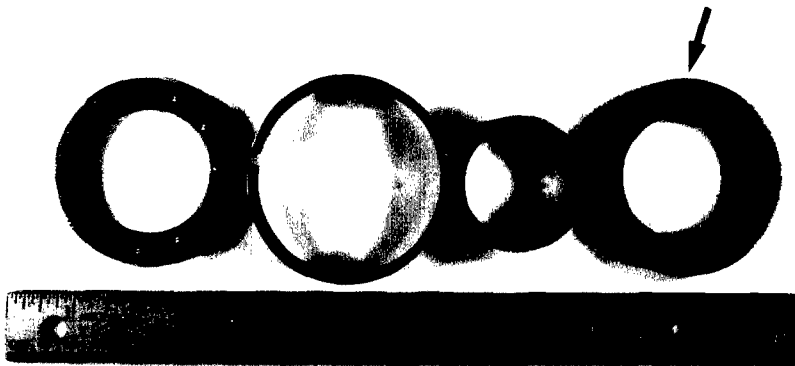


Figure 7. Overall view of the disassembled "Power Lock". The arrow is pointing to the crack in Ring A.

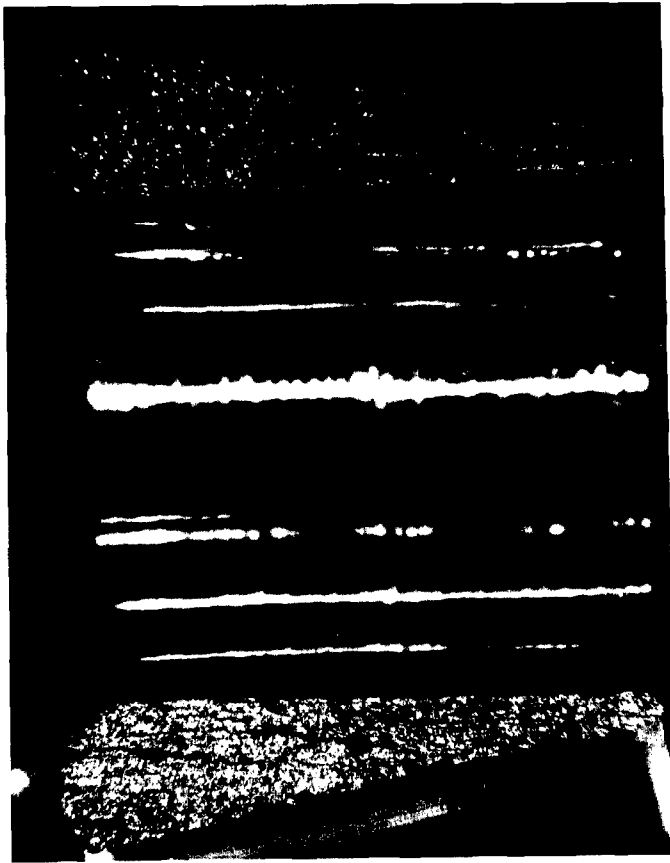


Figure 8. Broken open crack.

Mag. 8X

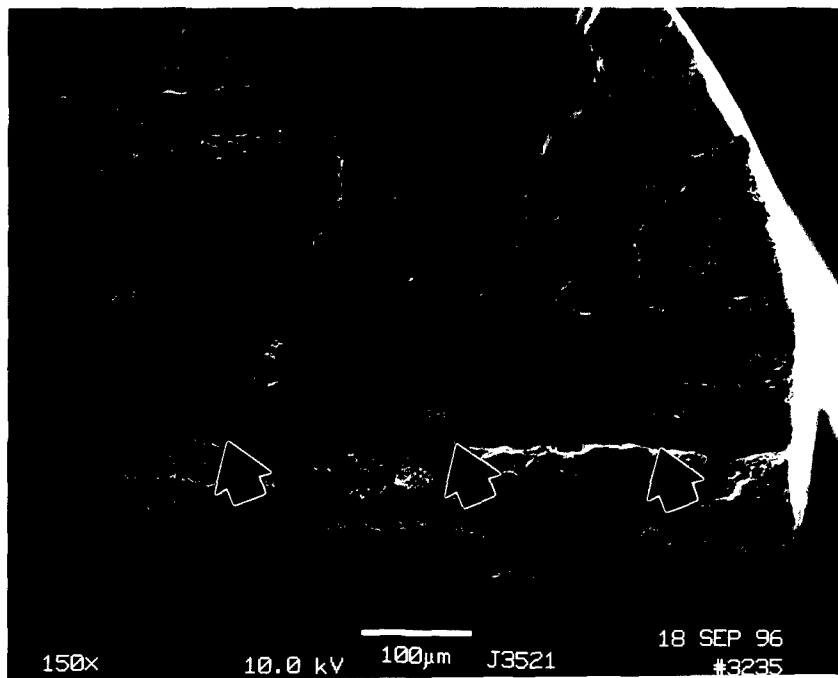


Figure 9. Higher magnification SEM fractograph reveals a long, smooth, flat area

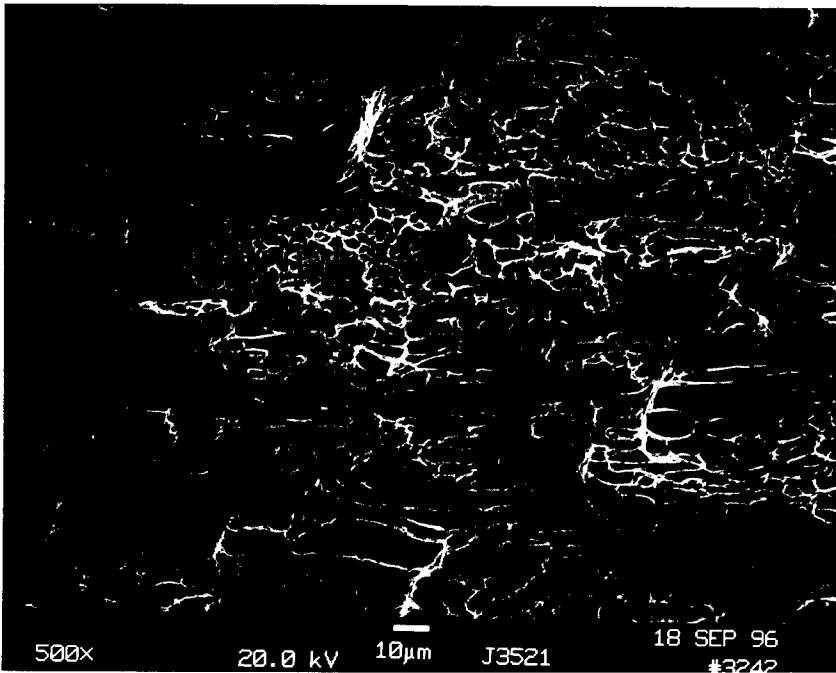


Figure 10. Ductile dimple rupture type of fracture observed in the “woody” areas of the fracture surface. Mag. 500X

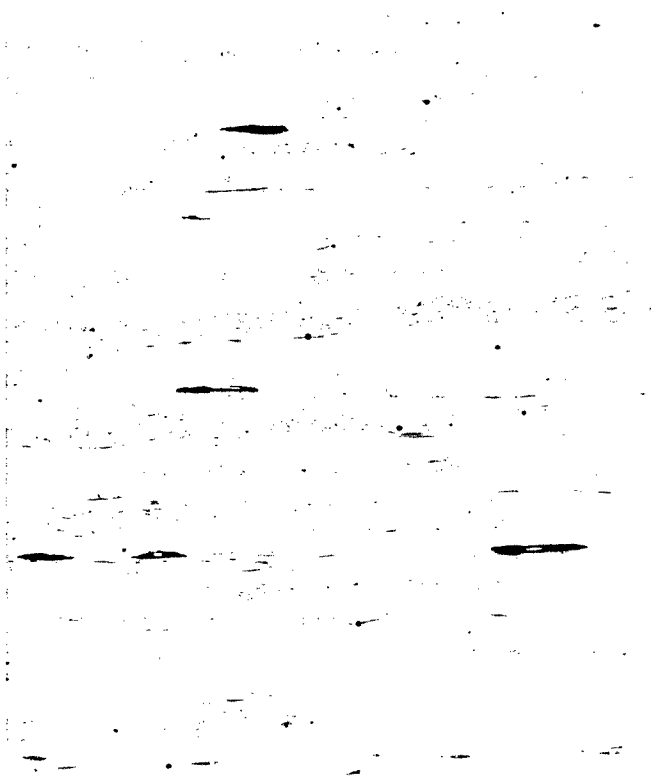


Figure 11. Mounted longitudinal cross-section through ring A showing manganese sulfide inclusions. As-polished. Mag. 100X